Distinct plasma-membrane PtdIns(4)*P* and PtdIns(4,5)P_2 dynamics in secretagogue-stimulated β-cells

Anne Wuttke, Jenny Sågetorp and Anders Tengholm*

Department of Medical Cell Biology, Uppsala University, Biomedical Centre, Box 571, SE-751 23 Uppsala, Sweden

*Author for correspondence (anders.tengholm@mcb.uu.se)

Accepted 7 February 2010
Journal of Cell Science 123, 1492-1502

doi:10.1242/jcs.060525

Summary

Phosphoinositides regulate numerous processes in various subcellular compartments. Whereas many stimuli trigger changes in the plasma-membrane PtdIns(4,5)P_2 concentration, little is known about its precursor, PtdIns(4)*P*, in particular whether there are stimulus-induced alterations independent of those of PtdIns(4,5)P_2. We investigated plasma-membrane PtdIns(4)*P* and PtdIns(4,5)P_2 dynamics in insulin-secreting MIN6 cells using fluorescent translocation biosensors and total internal reflection microscopy. Loss of PtdIns(4,5)P_2 induced by phospholipase C (PLC)-activating receptor agonists or stimulatory glucose concentrations was paralleled by increased PtdIns(4)*P* levels. In addition, glucose-stimulated cells regularly showed anti-synchronous oscillations of the two lipids. Whereas glucose-induced PtdIns(4)*P* elevation required voltage-gated Ca^{2+} entry and was mimicked by membrane-depolarizing stimuli, the receptor-induced response was Ca^{2+} independent, but sensitive to protein kinase C (PKC) inhibition and mimicked by phorbol ester stimulation. We conclude that glucose and PLC-activating receptor stimuli trigger Ca^{2+}- and PKC-dependent changes in the plasma-membrane PtdIns(4)*P* concentration that are independent of the effects on PtdIns(4,5)P_2. These findings indicate that enhanced formation of PtdIns(4)*P*, apart from ensuring efficient replenishment of the PtdIns(4,5)P_2 pool, might serve an independent signalling function by regulating the association of PtdIns(4)*P*-binding proteins with the plasma membrane.

Key words: Ca^{2+}, Glucose, Insulin-secreting cells, Oscillations, PI4-kinase, PtdIns(4)*P*, PtdIns(4,5)P_2

Introduction

Phosphoinositide lipids are minor components of all eukaryotic cell membranes. Seven different derivatives can be formed by phosphorylation of phosphatidylinositol (PtdIns) at the D-3, D-4 and D-5 positions of the inositol ring. In spite of their low abundance, phosphoinositides are important in many cellular processes. For example, the phosphoinositide 3-kinase (PI3K)-induced phosphorylation of phosphatidylinositol-4,5-bisphosphate [PtdIns(4,5)P_2] leads to increased levels of phosphatidylinositol-3,4,5-trisphosphate [PtdIns(3,4,5)P_3] and membrane recruitment of signalling proteins important for gene expression, cell proliferation and vesicle trafficking (Cantley, 2002). Another well-characterized example is the phospholipase C (PLC)-mediated hydrolysis of PtdIns(4,5)P_2 to inositol-1,4,5-trisphosphate [Ins(1,4,5)P_3] and diacylglycerol (DAG), leading to the mobilization of Ca^{2+} from intracellular stores and activation of protein kinase C (PKC), respectively (Berridge and Irvine, 1984). Receptor activation and other stimuli have been found to induce significant reduction in the plasma-membrane concentration of PtdIns(4,5)P_2 (Stauffer et al., 1998; Varnai and Balla, 1998). Changes of this lipid exert a signalling function of its own, regulating, for example, vesicle trafficking and cytoskeletal rearrangements (Czech, 2003; Yin and Janmey, 2003).

The PtdIns(4,5)P_2 pools are replenished by phosphorylation of phosphatidylinositol-4-phosphate [PtdIns(4)*P*] at the D-5 position by phosphatidylinositol 4-phosphate 5-kinases (PIP5Ks) (Fruman et al., 1998). PtdIns(4)*P* in turn is synthesized from PtdIns by phosphatidylinositol 4-kinases (PI4Ks) (Balla and Balla, 2006). There are two classes of mammalian PI4Ks (type II and type III), each with two isoforms (α and β), and three classes of PIP5Ks. PI4K type IIIα has been found to control the hormone-sensitive pool of PtdIns(4)*P* in the plasma membrane (Balla et al., 2008; Balla et al., 2005) and PI4K IIIβ has been suggested to be required for exocytosis in different types of cells (de Barry et al., 2006; Gromada et al., 2005; Kapp-Barnea et al., 2003). Silencing of PI4K IIIβ inhibits insulin secretion from INS1E and MIN6 β-cells (Waselle et al., 2005). Also, it has been shown that PtdIns(4)*P* potentiates Ca^{2+}-induced exocytosis in voltage-clamped mouse β-cells (Olsen et al., 2003) and permeabilized INS1E cells (Waselle et al., 2005). Some of these effects might be indirect and reflect the requirement for PtdIns(4,5)P_2 formed from PtdIns(4)*P*, but evidence is accumulating that PtdIns(4)*P* has direct regulatory effects in cells apart from its role as a PtdIns(4,5)P_2 precursor (Hama et al., 1999; Walch-Solimena and Novick, 1999). Most attention has been paid to PtdIns(4)*P* in intracellular membrane compartments, where the lipid regulates adaptor and coat-protein complexes as well as lipid-transfer proteins (D'Angelo et al., 2008). However, recent studies indicate that the majority of PtdIns(4)*P* resides in the plasma membrane (Hammond et al., 2009), but little is known about the regulation of PtdIns(4)*P* in this compartment. Studies in COS-7 cells expressing fluorescent-protein-tagged pleckstrin homology (PH) domains have demonstrated that PtdIns(4)*P* is formed in the plasma membrane during the recovery phase following activation of PLC by a Ca^{2+} ionophore (Balla et al., 2005). More recently, it was demonstrated that activation of heterologously expressed angiotensin II receptors induced a reduction in PtdIns(4)*P* concentration closely resembling that of PtdIns(4,5)P_2 (Balla et al., 2008). Activation of PLC is indeed

expected to reduce PtdIns(4)*P* levels, partly because PLC uses this lipid as substrate (Rhee and Choi, 1992) and partly because PtdIns(4)*P* is used to resynthesize PtdIns(4,5)P_2.

In this study, we employed total internal reflection fluorescence (TIRF) microscopy and lipid-binding fluorescent translocation biosensors for the real-time monitoring of PtdIns(4)*P* and PtdIns(4,5)P_2 dynamics in the plasma membrane of individual insulin-secreting MIN6 β-cells. Contrary to the view that the PtdIns(4)*P* concentration closely follows that of PtdIns(4,5)P_2, we now demonstrate that PLC-activating receptor stimuli and glucose, the major stimulator of insulin secretion from β-cells, trigger pronounced PKC- and Ca^{2+}-dependent increases in the plasma-membrane PtdIns(4)*P* concentration, paralleling the stimulus-evoked decrease in PtdIns(4,5)P_2. These observations emphasize the distinct regulation of the two phosphoinositides in the plasma-membrane compartment.

Results

Single-cell imaging of plasma-membrane PtdIns(4)*P* dynamics

Insulin-secreting MIN6 β-cells were transfected with the cyan fluorescent protein (CFP)-tagged PH domain from four phosphate adaptor protein 1 (FAPP1$_{PH}$-CFP) or from oxysterol-binding protein (OSBP$_{PH}$-CFP), both of which have a high in vitro binding affinity for PtdIns(4)*P* (Dowler et al., 2000; Levine and Munro, 1998). When analyzed with confocal microscopy, these biosensors showed diffuse distribution in the cytoplasm and distinct localization to intracellular membranes, probably the Golgi apparatus (Fig. 1A, upper row; supplementary material Fig. S1A). OSBP$_{PH}$-CFP was also found in the nucleus (Fig. 1A, upper row) and, in some cases, the construct showed faint plasma-membrane localization. Release of unbound cytoplasmic biosensor by digitonin permeabilization of the plasma membrane revealed marked plasma-membrane

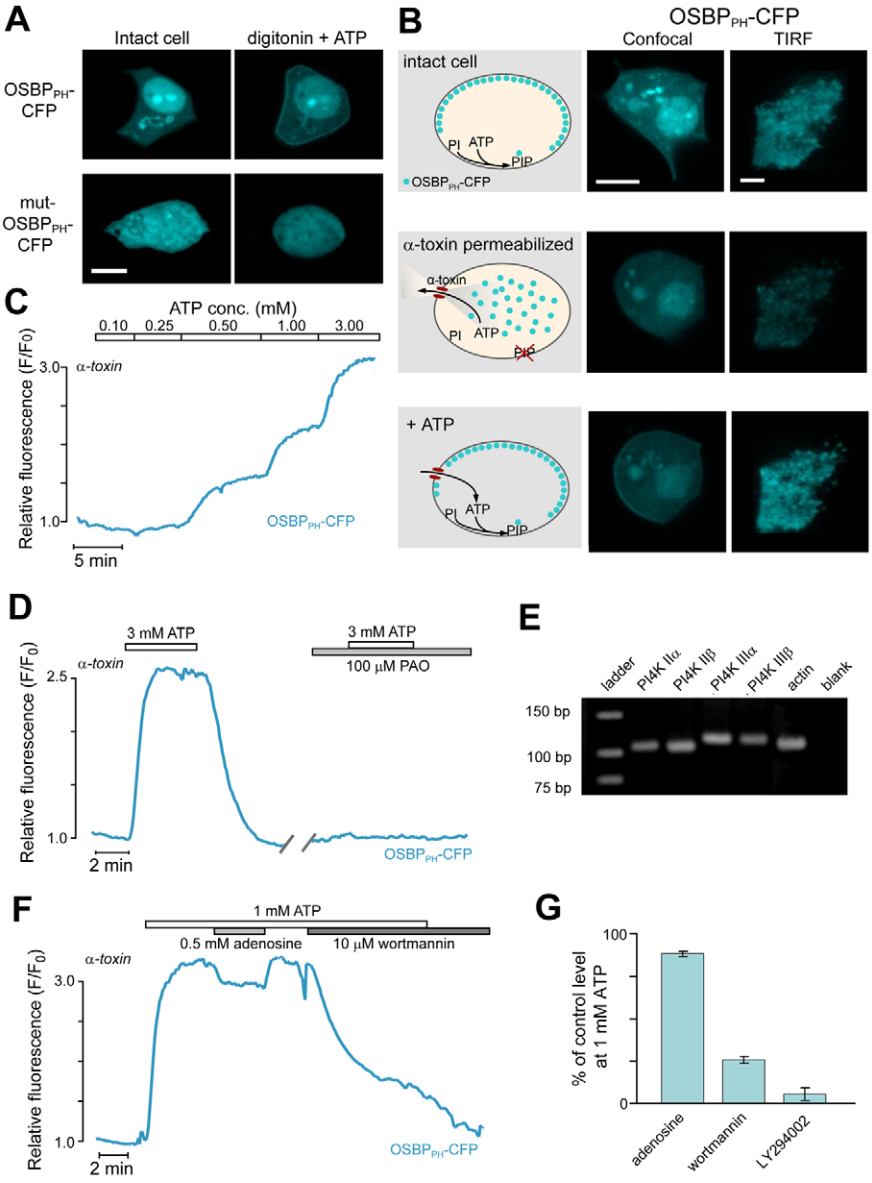

Fig. 1. Single-cell imaging of plasma-membrane PtdIns(4)*P* with OSBP$_{PH}$-CFP. (**A**) Confocal images of MIN6 β-cells expressing OSBP$_{PH}$-CFP (upper row; *n*=13) or PtdIns(4)*P*-binding-deficient mutOSBP$_{PH}$-CFP (lower row; *n*=9). The plasma-membrane localization of OSBP$_{PH}$-CFP becomes obvious after wash out of unbound probe from the cytoplasm by permeabilizing the plasma membrane with 20 μM digitonin in intracellular-like solution containing 3 mM ATP. Scale bar: 5 μm. (**B**) Membrane permeabilization with α-toxin results in the loss of small compounds such as ATP, but retains cytoplasmic biosensor. The lack of fuel leads to dissociation of the probe from the plasma membrane and subsequent addition of ATP causes PtdIns(4)*P*-dependent membrane association of OSBP$_{PH}$-CFP. Schematic drawing (left column) and images obtained with confocal (middle) and TIRF (right) microscopy. PI and PIP denote PtdIns and PtdIns(4)*P*, respectively. Scale bar: 5 μm. (**C**) TIRF microscopy recording of the ATP-dependent membrane translocation of OSBP$_{PH}$-CFP in an individual α-toxin-permeabilized MIN6 β-cell; *n*=22. (**D**) The ATP-dependent translocation of OSBP$_{PH}$-CFP recorded with TIRF microscopy in a single permeabilized cell is sensitive to PI4K inhibition with phenylarsine oxide (PAO; *n*=30). (**E**) RT-PCR analysis of the expression of PI4Ks in MIN6 β-cells. (**F**) Different effects of type II and type III PI4K inhibitors on ATP-dependent OSBP$_{PH}$-CFP translocation in a single permeabilized MIN6 β-cell. (**G**) Means ± s.e.m. for the effects of adenosine (*n*=25), wortmannin (*n*=25) and LY294002 (*n*=12) in experiments similar to that shown in F.

localization of the fluorescent construct (Fig. 1A, upper right). The fluorescence signal gradually disappeared within approximately 5 minutes after permeabilization, as the membrane-bound biosensor pool was washed away. To verify that the $OSBP_{PH}$-CFP localization reflected phophoinositide binding, a PH domain with much reduced affinity for PtdIns(4)*P* was created by changing arginines 107 and 108 to glutamates (mut$OSBP_{PH}$-CFP; Levine and Munro, 1998). This mutant PH domain showed homogenous cytoplasmic distribution without apparent membrane localization, even after digitonin permeabilization (Fig. 1A, lower row).

We next investigated PtdIns(4)*P* turnover using an approach with cells permeabilized by α-toxin from *Staphylococcus aureus* that was previously used in studies of PtdIns(4,5)P_2 (Thore et al., 2007). In contrast to digitonin, which causes release of large intracellular proteins, α-toxin creates small pores that only allow passage of molecules smaller than ~3 kDa. Permeabilization of MIN6 cells in an intracellular-like medium lacking ATP caused dissociation of $OSBP_{PH}$-CFP from the plasma membrane, reflecting the decrease in PtdIns(4)*P* concentration when PI4Ks became inactive because of the lack of substrate. Restoration of lipid kinase activity by addition of 1 mM ATP caused retranslocation of the biosensor to the plasma membrane (Fig. 1B, left and middle columns).

To measure fluorescence selectively at the plasma membrane, we employed TIRF microscopy, which excites fluorescent molecules exclusively in a small volume within ~100 nm of the membrane adhering to the coverslip, thereby minimizing the background from compartments deeper in the cell (Steyer and Almers, 2001; Axelrod, 2008). Intact MIN6 β-cells expressing $OSBP_{PH}$-CFP showed strong membrane fluorescence when imaged with TIRF microscopy. The dissociation of the probe from the membrane upon permeabilization and ATP-induced reassociation were detected as decreases and increases in CFP fluorescence, respectively (Fig. 1B, right column). Application of 1 mM ATP resulted in a 125±8% increase in fluorescence within 3 minutes (n=87). The effect of ATP was dose dependent, with translocation observed in the range from 0.25 mM (6 out of 22 cells) to 3 mM (all 22 cells; Fig. 1C), corresponding to physiological cytoplasmic concentrations of the nucleotide. Higher concentrations of ATP did not further increase the fluorescence signal (data not shown). The ATP-induced translocation of $OSBP_{PH}$-CFP in permeabilized cells was dependent on PI4K activity; 100 μM of the general PI4K inhibitor phenylarsine oxide completely prevented plasma-membrane localization of the construct (Fig. 1D). In separate control experiments, repeated applications of ATP evoked responses every time (data not shown). Reverse transcriptase PCR (RT-PCR) analysis of MIN6 β-cells demonstrated the presence of mRNA for all of the four known mammalian PI4K isoforms: type IIα and β and type IIIα and β (Fig. 1E). Different inhibitors were used to determine which of the PI4K subtypes are involved in plasma-membrane PtdIns(4)*P* production. Submillimolar concentrations of adenosine inhibit type II PI4K with little effect on the type III isoforms, whereas the well-known PI3K inhibitors wortmannin and LY294002 also act as type III PI4K inhibitors at high concentrations (Balla and Balla, 2006; Nakanishi et al., 1995). In the MIN6 β-cells, 0.5 mM adenosine had rather modest effects on the plasma-membrane PtdIns(4)*P* levels, whereas 10 μM wortmannin and 200 μM LY294002 strongly inhibited PtdIns(4)*P* formation (Fig. 1F,G).

Although $FAPP1_{PH}$-CFP was not clearly localized to the plasma membrane when analyzed with confocal microscopy, TIRF microscopy revealed strong membrane fluorescence, which decreased upon α-toxin permeabilization and increased dose dependently after subsequent introduction of ATP (supplementary material Fig. 1A,B). At low ATP concentrations (≤1 mM), biosensor translocation was more frequently observed in cells expressing $OSBP_{PH}$-CFP than in those expressing $FAPP1_{PH}$-CFP (P<0.001, n=22 and 20, respectively; supplementary material Fig. S1C), consistent with the higher affinity of the OSBP PH domain for PtdIns(4)*P* (Levine and Munro, 2002). Therefore, continued experiments were performed with $OSBP_{PH}$-CFP, but the most important findings were confirmed with $FAPP1_{PH}$-CFP.

Simultaneous recordings reveal differences in PtdIns(4,5)P_2 and PtdIns(4)*P* turnover

The PH domain of PLCδ1 is a well-established probe of membrane PtdIns(4,5)P_2 dynamics (Stauffer et al., 1998; Varnai and Balla, 1998; Xu et al., 2003). The YFP-tagged version ($PLC\delta1_{PH}$-YFP) was therefore used together with $OSBP_{PH}$-CFP or $FAPP1_{PH}$-CFP for simultaneous measurement of PtdIns(4,5)P_2 and PtdIns(4)*P*. Such dual-channel imaging demonstrated that PtdIns(4)*P* levels always increased before those of PtdIns(4,5)P_2 in α-toxin-permeabilized MIN6 β-cells upon readdition of ATP (time difference 31±4 seconds, n=22; Fig. 2A). Moreover, the results showed that, at low ATP concentrations, PtdIns(4)*P* could be generated without concomitant formation of PtdIns(4,5)P_2. Accordingly, 20 out of 79 cells responded to 0.25-1 mM ATP with an increase in PtdIns(4)*P* without change in PtdIns(4,5)P_2 until the ATP concentration was further increased (Fig. 2B). By contrast, ATP had little effect on the fluorescence from PtdIns(4)*P*-binding-deficient mut$OSBP_{PH}$-CFP, whereas the same cells showed a normal PtdIns(4,5)P_2 response (Fig. 2C,D). Because the PH domain of PLCδ1 shows a higher in vitro affinity for PtdIns(4,5)P_2 than $OSBP_{PH}$ does for PtdIns(4)*P* (Levine and Munro, 2002) and the two lipids are believed to be present at approximately equimolar concentrations (Lemmon, 2008), it seems unlikely that the time difference merely reflects different kinetic properties of the sensors or that the $OSBP_{PH}$-CFP signal is contaminated by crossreactivity with PtdIns(4,5)P_2 (Levine and Munro, 1998). Instead, the results indicate that PtdIns(4,5)P_2 is not formed without prior generation of PtdIns(4)*P*.

Inhibition of PI4K activity not only affected PtdIns(4)*P* levels, but also abolished the synthesis of PtdIns(4,5)P_2, in accordance with previous observations with phenylarsine oxide (Thore et al., 2007). When 200 μM LY294002 was added during the ATP-induced increase in the concentration of the phosphoinositides, the PtdIns(4)*P* levels immediately decreased, whereas those of PtdIns(4,5)P_2 started to decline after a delay of 25±4 seconds (Fig. 2E; P<0.001; n=9). Similar results were obtained when PI4K was inhibited at steady state (Fig. 2F for LY294002; wortmannin data not shown). Curve fitting to the data revealed that the decline of PtdIns(4,5)P_2 followed monoexponential kinetics (τ=291±47 seconds, n=9), whereas that of PtdIns(4)*P* was better described by a biexponential function (τ=34±4 seconds and 395±139 seconds, n=11; P<0.01 when comparing the chi square values as goodness-of-fit of a monoexponential versus a biexponential function). The fast and slow components accounted for about equal amplitudes of the overall decline. Together, these data indicate that there is high turnover of PtdIns(4)*P* and PtdIns(4,5)P_2 in the plasma membrane, that type III PI4K is crucial for maintaining the levels of both lipids, and that PtdIns(4,5)P_2 is synthesized by phosphorylation of the D5-position of PtdIns(4)*P*, rather than by alternative routes.

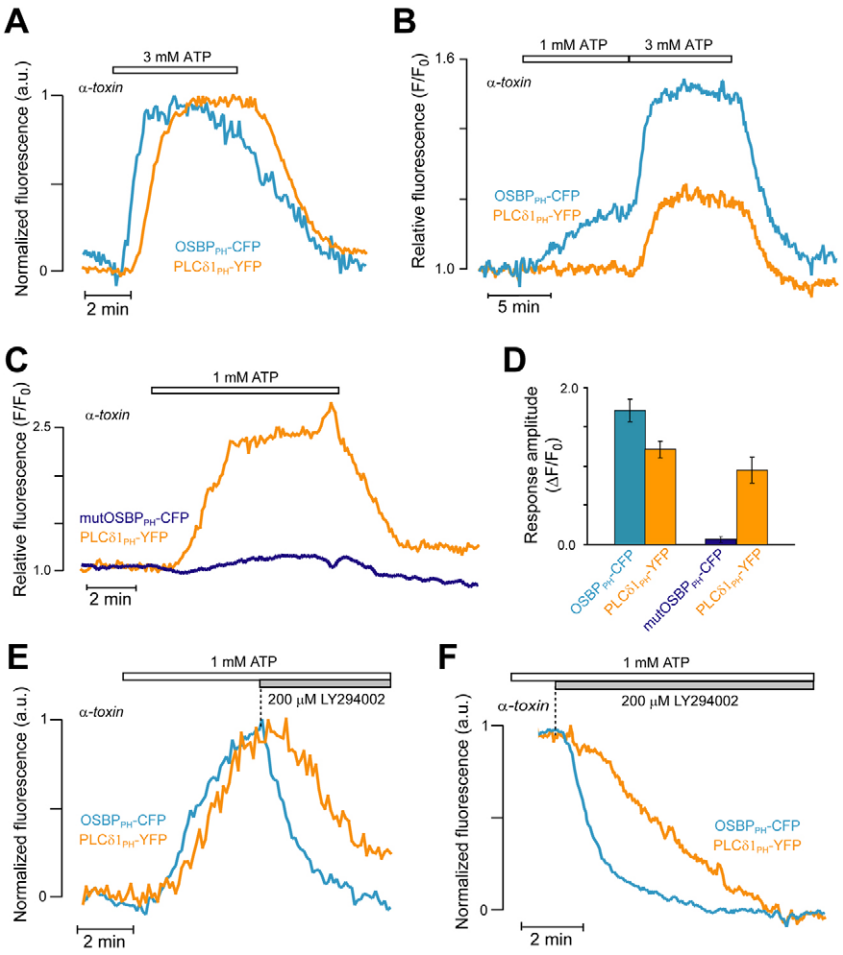

Fig. 2. Simultaneous recordings reveal differences in PtdIns(4)*P* and PtdIns(4,5)P_2 turnover. TIRF microscopy recordings of OSBP$_{PH}$-CFP (blue) and PLCδ1$_{PH}$-YFP (orange) fluorescence in individual α-toxin-permeabilized MIN6 β-cells exposed to 1-3 mM ATP. (**A**) ATP-induced translocation of OSBP$_{PH}$-CFP precedes that of PLCδ1$_{PH}$-YFP; *n*=22. (**B**) OSBP$_{PH}$-CFP sometimes translocates at lower ATP concentrations than PLCδ1$_{PH}$-YFP. Representative of 20 out of 79 cells. (**C**) ATP has little effect on mutOSBP$_{PH}$-CFP translocation. (**D**) Means ± s.e.m. for the biosensor translocation induced by 1 mM ATP in cells cotransfected with PLCδ1$_{PH}$-YFP and OSBP$_{PH}$-CFP (*n*=19) or mutOSBP$_{PH}$-CFP (*n*=9). (**E**,**F**) Dissociation of OSBP$_{PH}$-CFP and PLCδ1$_{PH}$-YFP from the plasma membrane following inhibition of type III PI4Ks by application of LY294002 during ATP-induced translocation (E; *n*=9) or at steady state (F; *n*=11). PLCδ1$_{PH}$-YFP dissociates after a delay and with different kinetics compared with OSBP$_{PH}$-CFP.

G_q-protein-coupled receptor stimulation elevates plasma-membrane PtdIns(4)*P* concentration

To investigate the relationship between PtdIns(4)*P* and PtdIns(4,5)P_2 in intact cells, MIN6 β-cells were challenged with 100 μM of the muscarinic agonist carbachol in the presence of a substimulatory glucose concentration (3 mM). As previously reported (Thore et al., 2005), carbachol activates PLC and induces a rapid decrease in plasma-membrane PLCδ1$_{PH}$-YFP fluorescence, followed by partial recovery to a sustained level and return to baseline after washout of the stimulus (Fig. 3A). In intact cells, the response kinetics of the PLCδ1 PH domain sensor are influenced by both membrane PtdIns(4,5)P_2 and the cytoplasmic concentration of Ins(1,4,5)P_3 (Xu et al., 2003). Dual recordings with PLCδ1$_{PH}$-YFP and OSBP$_{PH}$-CFP revealed that the decrease in PtdIns(4,5)P_2 is paralleled by increased concentrations of PtdIns(4)*P* (Fig. 3A). To simplify quantification and minimize the possible influence of nonspecific changes in membrane fluorescence induced by alterations in, for example, cell volume or attachment, the cells were cotransfected with OSBP$_{PH}$-CFP and YFP targeted to the plasma membrane by a palmitoylation and myristoylation motif (PM-YFP). When the ratio of CFP to YFP fluorescence was recorded, carbachol induced a 13±1% increase in the fluorescence ratio (*n*=52). This effect was completely reversed after inhibition of type III PI4Ks with 200 μM LY294002 (Fig. 3B). The fluorescence increase was specific, because it was also observed with FAPP1$_{PH}$-CFP (supplementary material Fig. S1D), but not with mutOSBP$_{PH}$-CFP, which does not bind PtdIns(4)*P* (Fig. 3C).

Previous studies in β-cells have indicated that Ca^{2+} released from intracellular stores and entering the cell through store-operated channels in the plasma membrane influences cellular phosphoinositide handling (Thore et al., 2005). Removal of extracellular Ca^{2+} and addition of 2 mM EGTA, in combination with depletion of intracellular Ca^{2+} stores with 50 μM of the sarco(endo)plasmic reticulum Ca^{2+}-ATPase inhibitor cyclopiazonic acid, consequently reduced both the initial transient and the subsequent sustained carbachol-induced PtdIns(4,5)P_2 response (P<0.001; Fig. 3D,E). By contrast, the Ca^{2+}-deficient conditions did not affect the corresponding PtdIns(4)*P* response (Fig. 3D,E). The stimulation of PtdIns(4)*P* synthesis was not unique to muscarinic receptors, because activation of purinergic receptors with 10 μM ATP induced a similar PtdIns(4)*P* elevation (Fig. 3F). By contrast, the PtdIns(4)*P* levels were unaffected by 100 nM glucagon (Fig. 3G) and stimulation with 100 nM insulin even caused a slight decrease in PtdIns(4)*P*. The latter effect was paralleled by pronounced activation of PI3K, detected as membrane translocation of the YFP-tagged PtdIns(3,4,5)P_3- and PtdIns(3,4)P_2-binding PH domain from Akt (YFP-Akt$_{PH}$) (Fig. 3H).

Receptor-induced PtdIns(4)*P* production depends on activation of PKC

To investigate whether signalling downstream of PLC feedback controls PtdIns(4)*P* levels, we exposed the cells to two consecutive pulses of carbachol in the absence or presence of inhibitors of PKC. Gö-6976, which inhibits conventional PKCs and protein

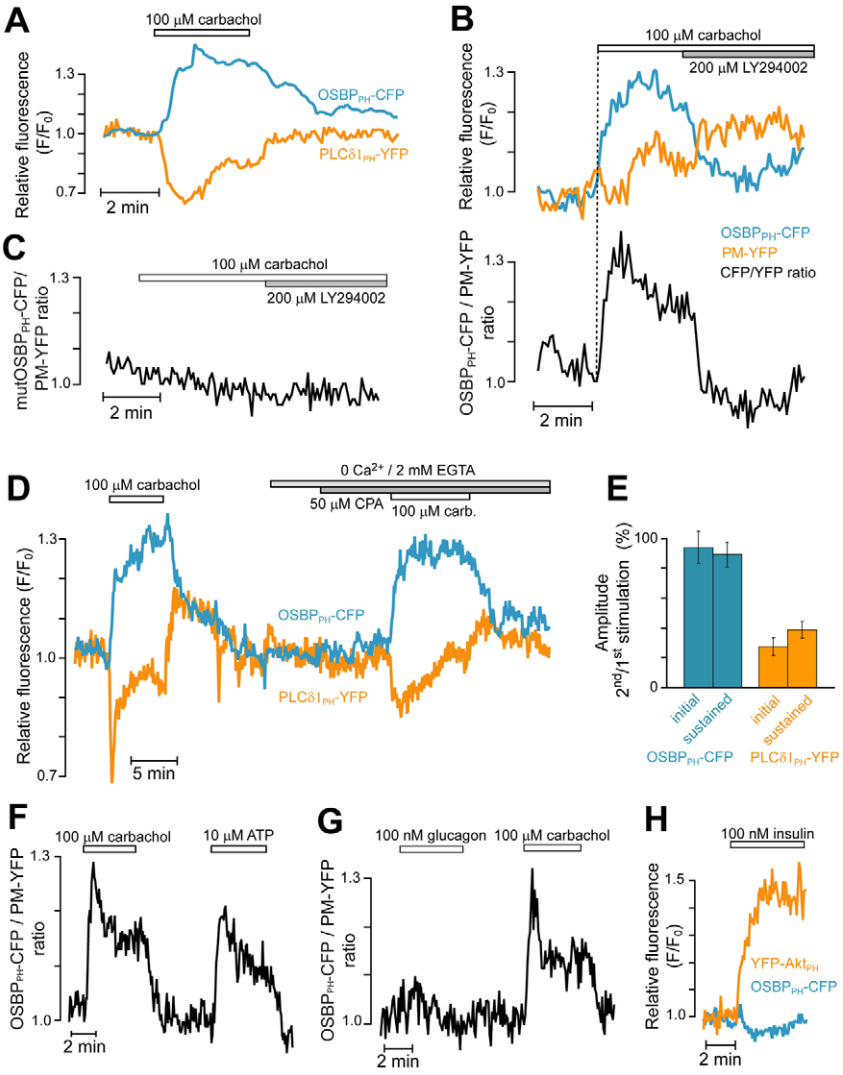

Fig. 3. Receptor-triggered loss of PtdIns(4,5)P_2 is associated with a rise in plasma-membrane PtdIns(4)P levels. (**A**) Simultaneous TIRF microscopy recordings of $OSBP_{PH}$-CFP (blue) and $PLC\delta1_{PH}$-YFP (orange) fluorescence in an intact MIN6 β-cell exposed to 100 μM carbachol; n=86. (**B**) Ratiometric TIRF recording of PtdIns(4)P (black, lower trace) during stimulation with carbachol. The original $OSBP_{PH}$-CFP (blue) and plasma-membrane-targeted YFP (PM-YFP; orange) recordings used to calculate the ratio are shown above. The response is reversed by inhibition of type III PI4Ks with 200 μM LY294002; n=23. (**C**) Carbachol and subsequent addition of LY294002 have no effect on the fluorescence ratio of PtdIns(4)P-binding-deficient $mutOSBP_{PH}$-CFP and PM-YFP; n=26. (**D**) Simultaneous TIRF recordings of PtdIns(4)P (blue) and PtdIns(4,5)P_2 (orange) showing that the carbachol-induced changes in the PtdIns(4)P levels are intact, whereas the PtdIns(4,5)P_2 response is reduced after exposure to 50 μM cyclopiazonic acid (CPA) in a Ca^{2+}-deficient medium containing 2 mM EGTA. (**E**) Mean ± s.e.m. for the effect of Ca^{2+}-deficient conditions on the carbachol response amplitude expressed as a percentage of the first control stimulation. n=23 for $OSBP_{PH}$-CFP, and 21 and 10 for the initial peak and sustained plateau responses of $PLC\delta1_{PH}$-YFP, respectively. (**F**,**G**) Ratiometric TIRF recordings of PtdIns(4)P concentration changes in response to 100 μM carbachol and 10 μM ATP (F; n=45) or 100 nM glucagon (G; n=11). (**H**) Parallel measurements of PtdIns(4)P with $OSBP_{PH}$-CFP and PtdIns(3,4,5)P_3 and PtdIns(3,4)P_2 with YFP-Akt_{PH} during stimulation with 100 nM insulin (n=29).

kinase D (PKD), but not novel PKCs, did not significantly affect the carbachol-induced PtdIns(4)P increase (Fig. 4A,D). By contrast, the related compound Gö-6983, which inhibits both conventional and novel PKC isoforms, but not PKD, markedly suppressed the carbachol effect (P<0.001; Fig. 4B,D). When Gö-6983 was present during the first carbachol stimulation, 8 out of 25 cells even showed a decrease in PtdIns(4)P (Fig. 4C), similar to the effect on PtdIns(4,5)P_2. Furthermore, when applied to non-stimulated cells in the presence of 3 mM glucose, 1 μM of the phorbol ester PMA (phorbol myristate acetate) triggered a prompt increase in PtdIns(4)P (21±1% increase in fluorescence ratio, n=50; Fig. 4E). As with carbachol, the PMA-induced PtdIns(4)P increase did not require elevation of the cytoplasmic Ca^{2+} concentration (Fig. 4E) and was inhibited by LY294002 (Fig. 4F,I) and Gö-6983 (Fig. 4G,I), but not by Gö-6976 (Fig. 4H,I). Together, these data indicate that receptor-stimulated PtdIns(4)P formation depends on PLC-mediated DAG formation with concomitant activation of PKC.

Glucose induces PtdIns(4)P oscillations in the plasma membrane

We next investigated how plasma-membrane PtdIns(4)P levels are affected by glucose, the major physiological stimulus of insulin secretion from pancreatic β-cells. Control experiments with PM-YFP showed that elevation of the glucose concentration from 3 to 11 mM often triggered an immediate increase in plasma-membrane fluorescence, probably due to a change in β-cell volume. Ratiometric measurements with $OSBP_{PH}$-CFP and PM-YFP revealed, however, a pronounced glucose-induced increase in the plasma-membrane PtdIns(4)P level (Fig. 5A; n=107), typically after a delay of 181±5 seconds. In some cells, this increase was transient (39%; Fig. 5A), whereas other cells showed a sustained (35%; Fig. 5B) or oscillatory (26%; Fig. 5C) response. In all cases, the glucose-induced PtdIns(4)P response was abolished by 200 μM LY294002 (Fig. 5D). Moreover, glucose had no effect on the CFP:YFP ratio in cells expressing $mutOSBP_{PH}$-CFP and PM-YFP (Fig. 5E). Glucose has previously been found to induce oscillations of the plasma-membrane PtdIns(4,5)P_2 concentration (Tamarina et al., 2005; Thore et al., 2007). Parallel recordings with $OSBP_{PH}$-CFP and $PLC\delta1_{PH}$-YFP demonstrated that the periodic peaks in the plasma-membrane concentration of PtdIns(4)P coincided with pronounced PtdIns(4,5)P_2 nadirs (Fig. 5F). Cross-correlation analysis revealed that the changes in PtdIns(4,5)P_2 preceded those in PtdIns(4)P by 5-10 seconds (Fig. 5G).

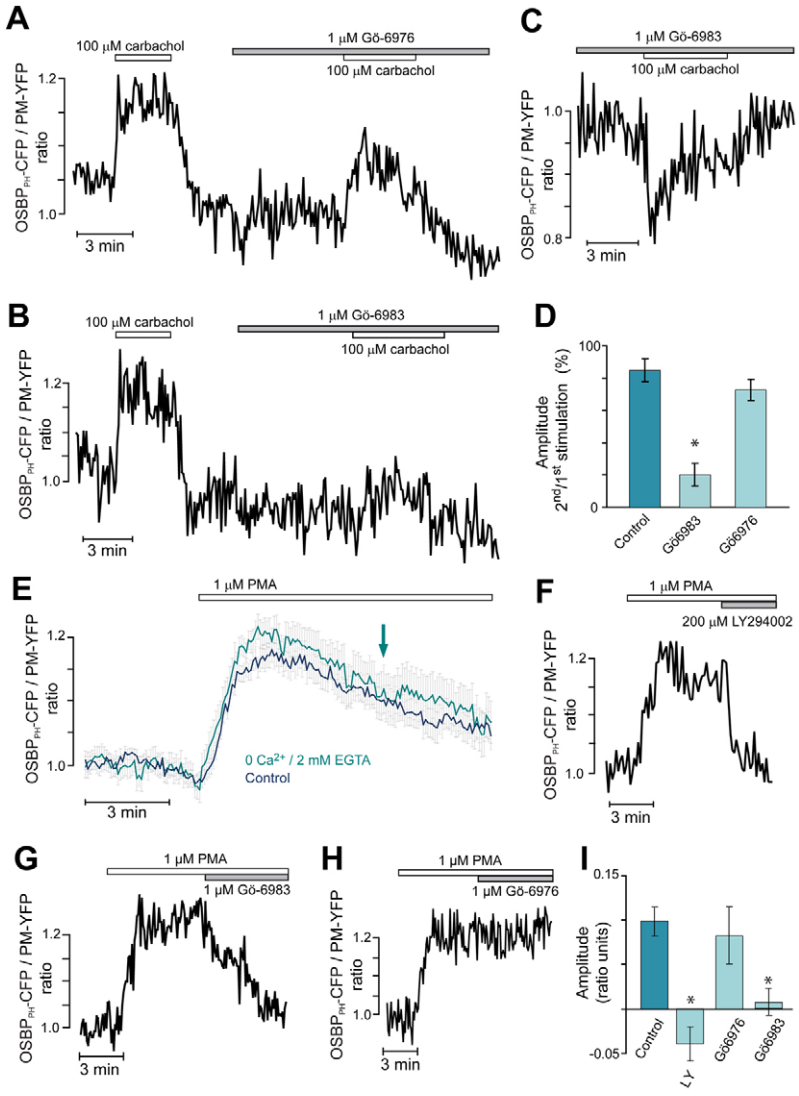

Fig. 4. Receptor-triggered increase in the plasma-membrane PtdIns(4)*P* concentration depends on the activation of PKC. (**A**) Ratiometric TIRF recording of PtdIns(4)*P* in response to 100 μM carbachol in the absence and presence of 1 μM of the PKC and PKD inhibitor Gö-6976; *n*=20 (**B**) Effect of the PKC inhibitor Gö-6983 on the carbachol-induced PtdIns(4)*P* response; *n*=17. (**C**) Example of a cell showing a carbachol-induced decrease in PtdIns(4)*P* in the presence of Gö-6983. Representative of 8 cells out of 25 without prior control stimulation. (**D**) Mean ± s.e.m. for the carbachol response amplitude, expressed as a percentage of the first control stimulation, in experiments performed as shown in A and B. *n*=14 (control with two consecutive carbachol additions without inhibitor), *n*=17 (Gö-6983) and *n*=20 (Gö-6976). **P*<0.001 for difference from control. (**E**) Mean ± s.e.m. for the elevation of membrane PtdIns(4)*P* concentration induced by PMA under control conditions (dark blue trace; *n*=27) and in Ca^{2+}-deficient medium containing 2 mM EGTA (light blue trace; *n*=17). Restoration of a physiological Ca^{2+} concentration (1.3 mM) in the latter medium is indicated by the arrow. (**F-H**) The PMA-induced PtdIns(4)*P* elevation is inhibited by LY294002 (F) and Gö-6983 (G), but not by Gö-6976 (H). (**I**) Mean ± s.e.m. for the effect of PMA-induced PtdIns(4)*P* responses in the presence of LY294002 and different PKC inhibitors expressed as the amplitude 10 minutes after stimulation (control) or 5 minutes after application of the test substance. *n*=7 for all inhibitors and *n*=27 for control. **P*<0.001 for difference from control.

The glucose-induced increase in plasma-membrane PtdIns(4)*P* concentration is Ca^{2+} dependent

The time delay between glucose stimulation and the PtdIns(4)*P* response, and the periodicity of the oscillations are reminiscent of the glucose-induced changes in the cytoplasmic Ca^{2+} concentration in β-cells (Grapengiesser et al., 1988). Measurements of PtdIns(4)*P* with $OSBP_{PH}$-CFP or $FAPP1_{PH}$-CFP in cells loaded with the fluorescent Ca^{2+} indicator Fura Red confirmed a strong link between the increases in PtdIns(4)*P* and the submembrane cytoplasmic Ca^{2+} concentration ($[Ca^{2+}]_{pm}$), with the change in Fura Red fluorescence preceding that of the PtdIns(4)*P* biosensor by 21±4 seconds (*n*=44; Fig. 6A; supplementary material Fig. S1E). The glucose-mediated increase in PtdIns(4)*P* was prevented by removal of extracellular Ca^{2+} as well as by hyperpolarization with 250 μM of the ATP-sensitive K^+ (K_{ATP}) channel opener diazoxide (Fig. 6B,C,E). Similarly, the response was much suppressed when L-type voltage-gated Ca^{2+} channels were inhibited with 50 μM methoxyverapamil (Fig. 6D,E). These data strongly indicate that the glucose effect on PtdIns(4)*P* is mediated by Ca^{2+}. Indeed, elevation of $[Ca^{2+}]_{pm}$ was sufficient to trigger an increase in PtdIns(4)*P*. Accordingly, membrane depolarization caused by closure of K_{ATP} channels with 1 mM tolbutamide or by elevation of the K^+ concentration to 30 mM triggered an increase in PtdIns(4)*P* of a magnitude similar to that induced by glucose (Fig. 6F-I). By contrast, 30 mM K^+ in the absence of extracellular Ca^{2+} had no effect (Fig. 6G,H), demonstrating that the increased PtdIns(4)*P* level was not secondary to membrane depolarization per se (Halaszovich et al., 2009). The K^+-depolarization-induced elevation of PtdIns(4)*P* was unaffected by both Gö-6983 and Gö-6976, indicating that $[Ca^{2+}]_{pm}$ regulates PtdIns(4)*P* by a mechanism independent of PKC and PKD (Fig. 6I,J).

Discussion

Single-cell measurements of plasma-membrane PtdIns(4)*P* dynamics

Although PtdIns(4)*P* has been implicated in the regulation of exocytosis and other cellular events, it is not known how the plasma-membrane concentration of the lipid changes upon physiological stimulation and how such changes are related to PtdIns(4,5)P_2. Studies of PtdIns(4)*P* dynamics in the plasma membrane have been limited by the lack of appropriate tools for single-cell measurements in this compartment. The PH domains of OSBP and FAPP1 have high in vitro binding specificities for PtdIns(4)*P* (Dowler et al., 2000; Levine and Munro, 1998). When

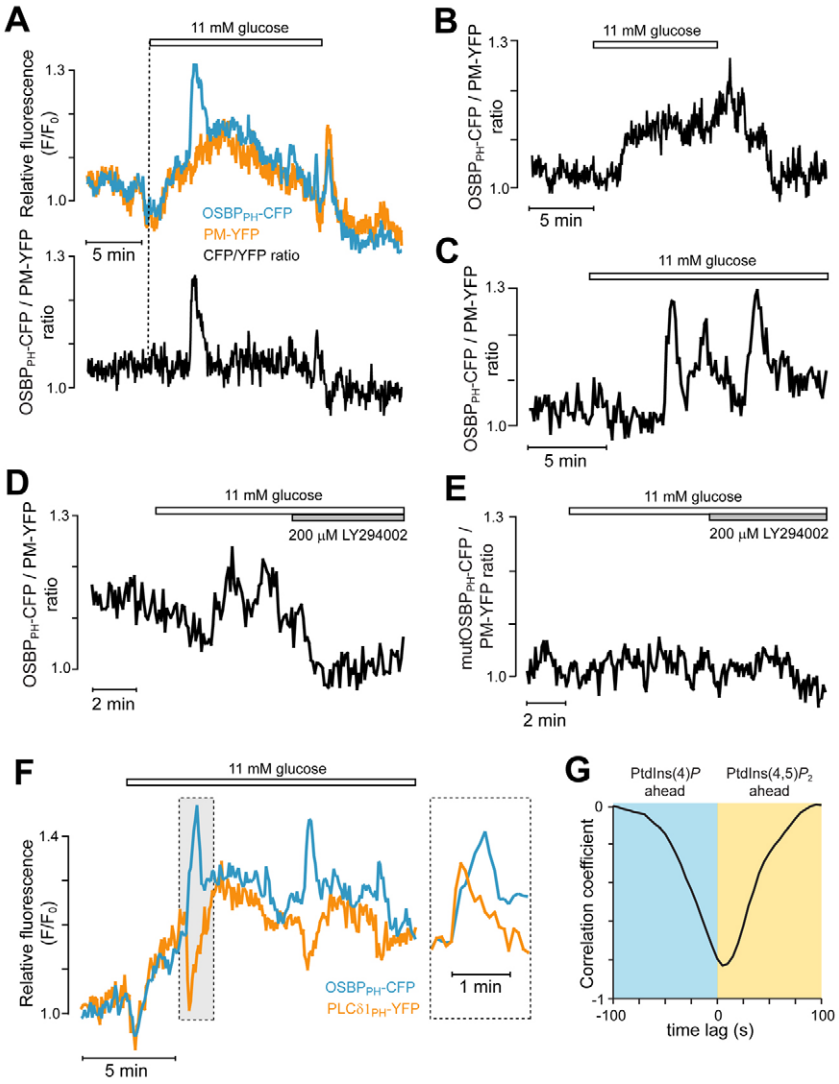

Fig. 5. Glucose triggers elevation of the plasma-membrane PtdIns(4)*P* concentration. (**A-C**) Ratiometric TIRF recordings of PtdIns(4)*P* (black traces) during elevation of the glucose concentration from 3 to 11 mM. The original $OSBP_{PH}$-CFP (blue) and PM-YFP (orange) recordings used to calculate the ratio are also shown in A. Glucose stimulation results in transient (A; *n*=41), sustained (B; *n*=37) or oscillatory (C; *n*=27) PtdIns(4)*P* responses. (**D**) Suppression of the glucose-induced PtdIns(4)*P* response by type III PI4K inhibition with 200 µM LY294002; *n*=6. (**E**) Ratiometric TIRF recording of PtdIns(4)*P*-binding-deficient $mutOSBP_{PH}$-CFP and PM-YFP during elevation of the glucose concentration from 3 to 11 mM and addition of LY294002; *n*=16. (**F**) Simultaneous TIRF recordings of $OSBP_{PH}$-CFP (blue) and $PLC\delta1_{PH}$-YFP (orange) fluorescence showing anti-synchronous glucose-induced oscillations of plasma-membrane PtdIns(4)*P* and PtdIns(4,5)P_2 levels. The boxed inset shows the part of the recording highlighted by a rectangle on an expanded time base and with the $PLC\delta1_{PH}$-YFP trace inverted to show that the change in PtdIns(4,5)P_2 reaches its maximum before that of PtdIns(4)*P*; *n*=4. (**G**) Cross-correlation of PtdIns(4)*P* and PtdIns(4,5)P_2 calculated from consecutive pairs of data segments of 100 seconds. The graph is an average correlogram of seven antiparallel peaks from four recordings of PtdIns(4)*P* and PtdIns(4,5)P_2 showing that the changes in PtdIns(4,5)P_2 precede those in PtdIns(4)*P*.

expressed as fluorescent protein fusions, they predominantly localize to the Golgi complex, which reflects binding to both PtdIns(4)*P* and the small GTPase Arf1 (Balla et al., 2005; Levine and Munro, 2002). In COS-7 cells, the sensors were found at the plasma membrane only during recovery after activation of PLC by a Ca^{2+} ionophore (Balla et al., 2005). More recently, the PH domain of the yeast OSH2 protein was identified as a PtdIns(4)*P*-binding protein (Yu et al., 2004) and used for confocal microscopy recordings of plasma-membrane PtdIns(4)*P* in yeast (Roy and Levine, 2004) and COS-7 cells (Balla et al., 2008), but the in vitro binding specificity for the lipid is relatively low (Yu et al., 2004). In this study, we show that the PH domains of OSBP and FAPP1 bind to the plasma membrane of insulin-secreting cells and that this membrane association is masked by a high background of free biosensor in the cytoplasm when analyzed with confocal microscopy. When plasma-membrane fluorescence was selectively monitored using TIRF microscopy, the sensors were found to undergo marked translocation to and from the membrane upon physiological stimulation. The specificity of $OSBP_{PH}$-CFP and $FAPP1_{PH}$-CFP for PtdIns(4)*P* was supported by the demonstration that the plasma-membrane localization was sensitive to inhibitors of PI4K and that a PtdIns(4)*P*-binding-deficient PH domain mutant failed to associate with the plasma membrane. Simultaneous measurements of PtdIns(4,5)P_2 with the well-characterized PH domain of PLCδ1, and PtdIns(3,4,5)P_3 and PtdIns(3,4)P_2 with that of Akt, showed that the PtdIns(4)*P* sensors responded with kinetics independent of that of the other phosphoinositide reporters.

Type III PI4Ks sustain plasma-membrane levels of PtdIns(4)*P* and PtdIns(4,5)P_2

Transcripts of all four known PI4K isoforms were present in the MIN6 cells. The observation that type III PI4Ks accounted for most PtdIns(4)*P* synthesis and maintenance of PtdIns(4,5)P_2 levels in the plasma membrane is consistent with findings in other cell types, in which type IIIα PI4K supports the hormone-sensitive pool of PtdIns(4)*P* and PtdIns(4,5)P_2 in this compartment (Balla et al., 2008; Balla et al., 2005; Nakanishi et al., 1995). The data are also in line with studies indicating that the type IIIβ isoform is important for exocytosis (de Barry et al., 2006; Gromada et al., 2005; Kapp-Barnea et al., 2003; Waselle et al., 2005), although the relative contributions of the α and β isoforms were not clarified in this work. The type III PI4Ks have mainly been found in organelle membranes (Balla et al., 2005; D'Angelo et al., 2008; Wiedemann et al., 1996) and it is unclear how rapid changes in PtdIns(4)*P* can take place in the plasma membrane unless a fraction of PI4K is at least transiently associated with this compartment. In PC12 cells,

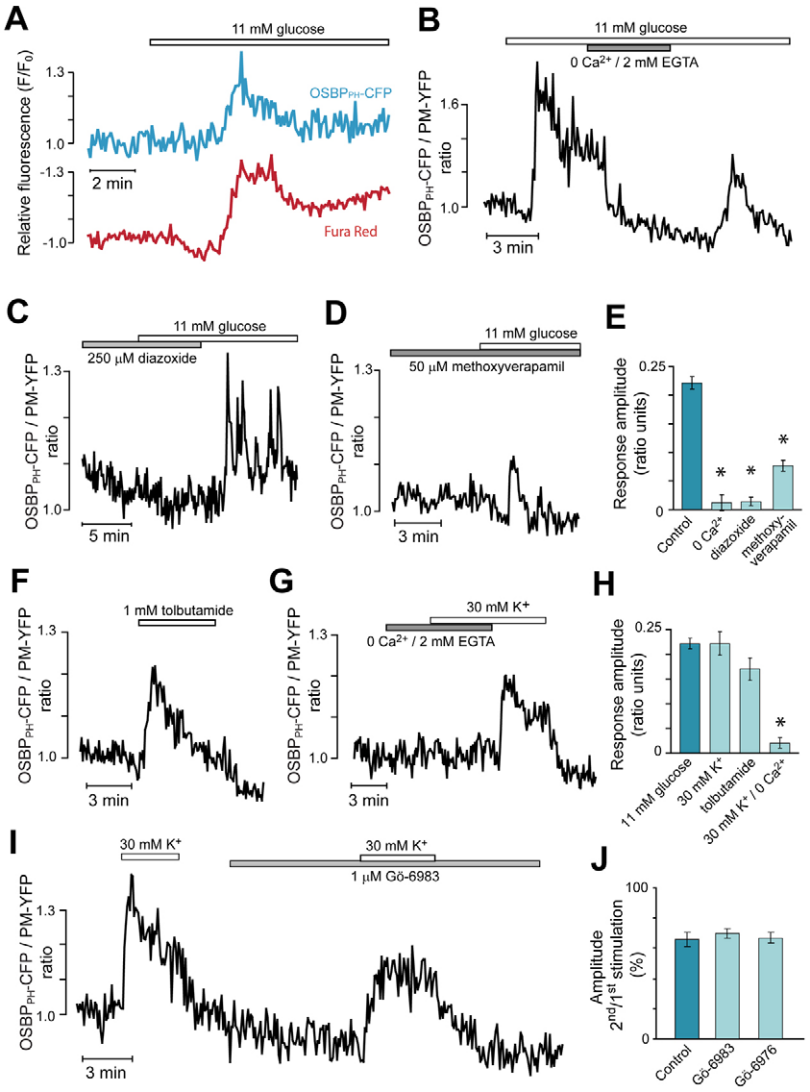

Fig. 6. The glucose-induced increase in PtdIns(4)*P* levels is mediated by depolarization-evoked elevation of the cytoplasmic Ca^{2+} concentration. (**A**) Simultaneous TIRF recordings of plasma-membrane PtdIns(4)*P* from $OSBP_{PH}$-CFP (blue) and cytoplasmic Ca^{2+} concentration in the submembrane space (red) in a Fura-Red-loaded MIN6 β-cell during elevation of the glucose concentration from 3 to 11 mM; *n*=5. (**B-D**) Ratiometric TIRF recordings of PtdIns(4)*P* from $OSBP_{PH}$-CFP and PM-YFP showing inhibition of the glucose-induced PtdIns(4)*P* response in a Ca^{2+}-deficient medium (B), by hyperpolarization with 250 μM diazoxide (C) or by inhibition of voltage-gated Ca^{2+} channels with 50 μM methoxyverapamil (D). (**E**) Mean ± s.e.m. for the effects of Ca^{2+} removal (*n*=24), diazoxide (*n*=21) and verapamil (*n*=41) on the PtdIns(4)*P* elevation induced by 11 mM glucose (control, *n*=56). **P*<0.001 for difference from control. (**F**,**G**) Ratiometric TIRF recordings of PtdIns(4)*P* showing the effect of depolarization-induced elevation of cytoplasmic Ca^{2+} concentration triggered by closure of ATP-sensitive K^+ channels with 1 mM tolbutamide (F) or by elevation of the extracellular K^+ concentration to 30 mM (G). The KCl response is prevented by removal of extracellular Ca^{2+}. (**H**) Mean ± s.e.m. for the PtdIns(4)*P* response amplitude induced by tolbutamide (*n*=7) or high K^+ in the presence (*n*=9) or absence (*n*=9) of extracellular Ca^{2+}. The response to glucose (*n*=56, control bar in E) is shown for comparison. **P*<0.001 for difference from 30 mM K^+. (**I**) The depolarization-induced PtdIns(4)*P* elevation is insensitive to the PKC inhibitor Gö-6983. (**J**) Mean ± s.e.m. for the effect of PKC inhibitors on KCl-induced PtdIns(4)*P* elevation. *n*=19 (control), *n*=23 (Gö-6983) and *n*=23 (Gö-6976).

PI4K has been found to translocate from intracellular sites to the membrane in response to depolarizing stimuli (de Barry et al., 2006). We did not determine the localization of PI4Ks in insulin-secreting cells, but it is interesting to note that the mechanism responsible for increasing PtdIns(4)*P* in the plasma membrane remains intact after permeabilization of the membrane.

Receptor-induced elevation of plasma-membrane PtdIns(4)*P* concentration

Activation of endogenous muscarinic and purinergic receptors triggered a marked increase in membrane PtdIns(4)*P* levels in insulin-secreting cells. This effect required type III PI4K activity, indicating that PtdIns(4)*P* is formed from PtdIns rather than by dephosphorylation of more highly phosphorylated phosphoinositides. The increased PtdIns(4)*P* concentration coincided with the reduction in PtdIns(4,5)P_2 and increase in Ins(1,4,5)P_3 levels that has previously been reported after activation of PLC (Tamarina et al., 2005; Thore et al., 2005; Thore et al., 2007), suggesting that PtdIns(4)*P* is not a prominent substrate of β-cell PLC isozymes. Our findings are in contrast to recent observations in COS-7 cells, in which activation of heterologously expressed angiotensin receptors caused a decrease in membrane PtdIns(4)*P* concentration, closely following the agonist-induced changes in PtdIns(4,5)P_2 (Balla et al., 2008). This discrepancy probably reflects the use of different cell types, because the present data from the insulin-secreting cell line are supported by the previous observation in mouse islet cells that carbachol increases the total radiolabelled PtdIns(4)*P* level through a PI4K-dependent mechanism (Kardasz et al., 1997).

The carbachol-induced PtdIns(4)*P* response did not require elevation of the cytoplasmic Ca^{2+} concentration and was not directly correlated with the changes in plasma-membrane PtdIns(4,5)P_2 concentration. However, based on the observation that the response was mimicked by phorbol ester and blocked by an inhibitor of novel PKC isoforms, we conclude that PtdIns(4)*P* levels are regulated by PKC (Fig. 7). Interestingly, when PKC was inhibited, carbachol sometimes triggered a decrease in PtdIns(4)*P*, resembling the results from Balla et al. (Balla et al., 2008). Type III PI4Ks in the Golgi compartment have been found to be regulated by DAG and PKD (Hausser et al., 2005), but in our hands carbachol-induced PtdIns(4)*P* formation was unaffected by an inhibitor of conventional PKC isoforms and PKD. Instead, the response was markedly suppressed by a closely related inhibitor of conventional and novel PKCs that has no effect on PKD. Phorbol esters and PKC have

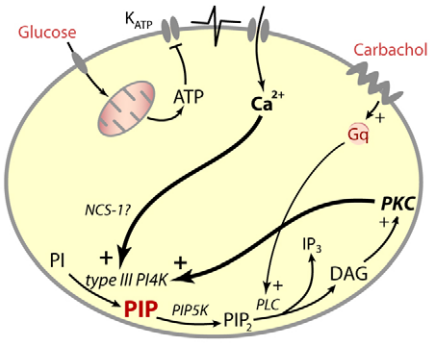

Fig. 7. Stimulus-induced increases in plasma-membrane PtdIns(4)*P* concentration in insulin-secreting cells. Glucose triggers elevation of PtdIns(4)*P* levels by a mechanism that involves K_{ATP}-channel-dependent membrane depolarization and voltage-gated Ca^{2+} influx. Ca^{2+} triggers PtdIns(4)*P* formation, possibly by activating the Ca^{2+}-binding protein NCS-1, which is known to activate type III PI4Ks. Stimulation of PLC through G_q-coupled muscarinic receptors, which can be activated by carbachol, results in elevation of the plasma-membrane PtdIns(4)*P* concentration through a mechanism that involves DAG-mediated activation of PKC. PI, PIP and PIP_2 are abbreviations for PtdIns, PtdIns(4)*P* and PtdIns(4,5)P_2, respectively.

been found to stimulate PtdIns(4)*P* generation in several different systems (Giraud et al., 1988; Halenda and Feinstein, 1984; Kardasz et al., 1997; Taylor et al., 1984) and future studies will clarify whether DAG-mediated PKC activation is a general mechanism regulating PI4K activity in the plasma membrane.

Glucose-induced PtdIns(4)*P* formation

In contrast to the receptor-triggered response, the glucose-induced increase in plasma-membrane PtdIns(4)*P* concentration required voltage-gated Ca^{2+} influx and elevation of the cytoplasmic Ca^{2+} concentration (Fig. 7). From the observation that PI4K was inhibited by ADP, it has been suggested that the enzyme acts as an ATP and ADP sensor in β-cells, stimulating the PtdIns(4)*P* production necessary for exocytosis in relation to metabolic demand (Olsen et al., 2003). In this study, ATP was indeed found to stimulate PtdIns(4)*P* formation in permeabilized cells, but in intact cells glucose had no effect on the plasma-membrane PtdIns(4)*P* pool unless the cytoplasmic Ca^{2+} concentration was allowed to increase. Indeed, elevation of the cytoplasmic Ca^{2+} concentration by depolarizing stimuli was sufficient to trigger a PtdIns(4)*P* response of similar magnitude to that triggered by glucose. Accordingly, the PtdIns(4)*P* oscillations probably reflect the characteristic slow oscillations of the cytoplasmic Ca^{2+} concentration in glucose-stimulated β-cells (Grapengiesser et al., 1988). The mechanism by which Ca^{2+} elevates the plasma-membrane PtdIns(4)*P* concentration in glucose-stimulated β-cells remains unclear. Increased levels of the cytoplasmic Ca^{2+} concentration activate PLC in β-cells (Biden et al., 1987; Thore et al., 2004), but in contrast to the carbachol-triggered PtdIns(4)*P* response, the response induced by $[Ca^{2+}]_{pm}$ elevation was unaffected by PKC inhibition. PI4K is an effector of the Ca^{2+}-binding protein neuronal calcium sensor-1 (NCS-1) (Hendricks et al., 1999; Zhao et al., 2001). NCS-1 is expressed in β-cells, and the interaction between NCS-1 and PI4K has been suggested to promote insulin granule exocytosis (Gromada et al., 2005). It is therefore tempting to speculate that glucose and depolarizing stimuli increase PtdIns(4)*P* by activating PI4Ks through NCS-1.

Significance of stimulus-induced increases in plasma-membrane PtdIns(4)*P*

A secretagogue-induced increase in PtdIns(4)*P* in the plasma membrane should have several functional implications. First, it will ensure fast resynthesis of PtdIns(4,5)P_2 in response to PLC activity. From the observation that the production rate of Ins(1,4,5)P_3 was much faster than the decline in PtdIns(4,5)P_2 levels in bradykinin-stimulated neuroblastoma cells, it was predicted that the synthesis of this lipid must be stimulated (Xu et al., 2003). Because PtdIns(4)*P* is the rate-limiting substrate for the production of PtdIns(4,5)P_2, increased availability of PtdIns(4)*P* would favour the production of higher phosphorylated inositide lipids. The PKC-mediated feedback stimulation of PtdIns(4)*P* synthesis might thus act to sustain the PtdIns(4,5)P_2 levels. Second, phosphoinositides are important in exocytosis by regulating the priming, docking and fusion of secretory granules (Hay et al., 1995; Martin, 2001; Olsen et al., 2003; Waselle et al., 2005; Wiedemann et al., 1996). Although most attention has been paid to the role of PtdIns(4,5)P_2 in this context, there is also evidence of stimulatory effects of PtdIns(4)*P* on exocytosis (Olsen et al., 2003). It is interesting to note that CAPS (Ca^{2+}-activated protein for secretion), an important mediator of PtdIns(4,5)P_2 action in exocytosis (Speidel et al., 2008), also binds to PtdIns(4)*P* (Loyet et al., 1998). Secretagogue-induced increases in membrane PtdIns(4)*P* levels might therefore be involved in priming of granules for exocytosis. In summary, we have investigated PtdIns(4)*P* and PtdIns(4,5)P_2 dynamics in the plasma membrane, and found that glucose and PLC-activating agonists trigger Ca^{2+}- and PKC-dependent changes in PtdIns(4)*P* distinct from those in PtdIns(4,5)P_2. The demonstration that PtdIns(4)*P*-binding proteins are recruited to the membrane in response to cell stimulation reinforces the idea that plasma-membrane PtdIns(4)*P* by itself can exert a second messenger function.

Materials and Methods

Reagents and DNA constructs

HEPES and BSA were from Roche Diagnostics (Bromma, Sweden), and diazoxide was a kind gift from Schering-Plough, Knoll AG (Germany). Unless otherwise stated, all other chemicals were purchased from Sigma-Aldrich (St Louis, MO, USA). The plasmids containing $OSBP_{PH}$-CFP and $FAPP1_{PH}$-CFP (Balla et al., 2005) were generously made available by Tamas Balla, National Institutes of Health, Bethesda, MD, USA. Phosphoinositide-binding-deficient $mutOSBP_{PH}$-CFP was created by introducing the mutations R107E and R108E into $OSBP_{PH}$-CFP by QuikChange mutagenesis, according to the manufacturer's protocol (Stratagene, La Jolla, CA, USA). The plasmids for the YFP-tagged PH domains of PLCδ1 (Stauffer et al., 1998) and Akt (Kontos et al., 1998), as well as for YFP targeted to the plasma membrane by palmitoylation and myristoylation (PM-YFP) (Teruel et al., 1999), were kindly provided by Tobias Meyer, Stanford University, CA, USA.

Cell culture and transfection

Insulin-secreting MIN6 β-cells (passage 17-30) (Miyazaki et al., 1990) were cultured in DMEM containing 25 mmol/l glucose and supplemented with 2 mmol/l glutamine, 70 μmol/l 2-mercaptoethanol, 100 units/ml penicillin, 100 μg/ml streptomycin and 15% fetal calf serum, and kept at 37°C in a humidified atmosphere with 5% CO_2. For transfection, ~200,000 cells were suspended in 100 μl Optimem medium containing 0.5 μg Lipofectamine 2000 (Invitrogen, Carlsbad, CA, USA) with up to 0.3 μg plasmid DNA and plated on a 25 mm polylysine-coated coverslip. After 3 hours, when the cells were attached, the transfection was interrupted by the addition of 3 ml complete cell culture medium. Experiments were conducted after 18-36 hours of culture.

Buffers and cell permeabilization

Before experiments, the cells were transferred to a buffer containing 125 mM NaCl, 4.8 mM KCl, 1.3 mM $CaCl_2$, 1.2 mM $MgCl_2$ and 25 mM HEPES with pH adjusted to 7.40 with NaOH, and incubated for 30 minutes at 37°C. For $[Ca^{2+}]_{pm}$ measurements, transfected cells were preincubated in the presence of 10 μM of the acetoxymethyl ester of the fluorescent Ca^{2+} indicator Fura Red (Molecular Probes Invitrogen), followed by washing in indicator-free buffer. Where indicated, the cells were permeabilized with digitonin or α-toxin from *S. aureus* (PhPlate Stockholm, Sweden). The cells were then superfused with an intracellular-like medium containing 140 mM

KCl, 6 mM NaCl, 1 mM $MgCl_2$, 0.465 mM $CaCl_2$, 0.1 mM EGTA and 10 mM HEPES with pH adjusted to 7.00 with KOH. Digitonin was added at a concentration of 20 μM, together with 3 mM Mg-ATP, until there was a sudden decrease in fluorescence intensity. For permeabilization with α-toxin, perifusion was temporarily interrupted and 5 μl α-toxin (0.46 mg/ml) was added directly into the 50 μl superfusion chamber. After 2 minutes, cells were washed and 0.1-3 mM Mg-ATP was added to the medium, while the concentrations of free Mg^{2+} and Ca^{2+} were maintained at 1 mM and 100 nM, respectively.

Fluorescence microscopy

The coverslips with the attached cells were used as exchangeable bottoms of an open 50 μl chamber and superfused with buffer at a rate of 0.3 ml/minute. All experiments were performed at 37°C. The subcellular distributions of the fluorescent biosensors were analyzed with a Yokogawa CSU-10 spinning disk confocal system (Andor Technology, Belfast, Northern Ireland) attached to a Diaphot 200 microscope (Nikon) with a 60× 1.40 NA objective (Nikon). CFP was excited at 442 nm with the light from a diode laser (Oxxius, Laser2000, Norrköping, Sweden) and the 514 nm line of an argon ion laser (ALC 60×, Creative Laser Corporation, Munich, Germany) was used to excite YFP. Appropriate wavelengths were selected with the help of an acousto-optic tunable filter (AA Optoelectronics, Orsay Cedex, France). The laser beam was homogenized and expanded by a rotating light-shaping diffuser (Physical Optics Corporation, Torrance, CA) before being refocused into the confocal scanhead.

An evanescent wave microscopy setup, consisting of an Eclipse Ti microscope (Nikon) with a TIRF illuminator (Nikon), was used for measurement of the plasma-membrane concentration of the fluorescent protein constructs. The 458 nm and 514 nm lines of an argon laser (Creative Laser Production, Munich, Germany) were selected by appropriate filters in a filter wheel (Sutter Instruments) and used to excite CFP and YFP or Fura Red, respectively. The beam was coupled to the TIRF illuminator through an optical fibre (Oz Optics, Ottawa, Canada). In both the confocal and TIRF microscope setups, fluorescence was detected with back-illuminated EMCCD cameras (DU-888 and DU-887, respectively, Andor Technology) under MetaFluor (Molecular Devices Corp., Downington, PA) software control. Emission wavelengths were selected with filters [485 nm/25 nm half-bandwidth for CFP, 560/40 nm for YFP (Semrock, Rochester, NY, USA) and 630 nm long pass for Fura Red (Melles-Griot, Didam, The Netherlands)] mounted in a filter wheel (Sutter Instruments). For time-lapse recordings, images or image pairs were acquired every 2-5 seconds. To minimize exposure of the cells to the potentially harmful laser light, the beam was blocked by the AOTF or a mechanical shutter (Sutter Instruments) between image captures.

RNA isolation and RT-PCR

Total RNA was extracted from MIN6 β-cells using the RNEasy mini kit (Qiagen). The first strand cDNA was generated using oligo-dT primers and the Superscript III First-Strand Synthesis System for RT-PCR kit (Invitrogen), according to the manufacturer's protocols. Specific cDNA sequences were amplified in a thermocycler (LightCycler, Roche) using 1 μM each of forward and reverse primers and Platinum PCR Supermix (Invitrogen). The primers for RT-PCR analysis were designed from the coding sequences of mouse genes as follows: PI4K type IIα, forward 5′- gaccaaaaactggaactcaa-3′, reverse 5′-ttgcccctggactttact-3′; PI4K type IIβ, forward 5′-ctaaccaggggtacctttct-3′, reverse 5′-gtctcactgacaagccaaa-3′; PI4K type IIIα, forward 5′-ccagtatggggatgagtcta-3′, reverse 5′-gtgcctgtccttgatctg-3′; PI4K type IIIβ, forward 5′-tgcttggtctgctacctatt-3′, reverse 5′-tgagctggaaaggatgaa-3′. The primer pairs were tested for self-complementarity, dimer formation and melting temperature using the Primer 3 software (Rozen and Skaletsky, 2000). Amplification consisted of 1 cycle of 1 minute at 95°C and 40 cycles of 10 seconds at 95°C, 10 seconds at 50°C and 8 seconds at 72°C. To assess integrity and quantity of the reverse transcribed RNA, the same cDNA samples were amplified with β-actin-specific primers (forward 5′-ggacctgactgactacctca-3′, reverse 5′-gcacagcttctccttaatgt-3′). Amplified products were controlled for length by ethidium bromide staining after electrophoresis on 1% agarose gels, and further analyzed by DNA sequencing and BLAST analysis against the GenBank database.

Data analysis

Image analysis was carried out using the ImageJ software (http://rsb.info.nih.gov/ij). Fluorescence intensities were expressed in relation to initial fluorescence after subtraction of background (F/F_0). Curve fitting and cross-correlation were performed with IGOR Pro (Wavemetrics, Lake Oswego, OR, USA) and MATLAB (The Mathworks, Natick, MA, USA) software, respectively. Data are presented as mean values ± s.e.m. and statistical analyses performed with Student's *t*-test.

We thank Tamas Balla and Tobias Meyer for generously providing expression plasmids. This study was supported by grants from Åke Wiberg's Foundation, the European Foundation for the Study of Diabetes/MSD, the Family Ernfors Foundation, Harald and Greta Jeanssons Foundations, Magnus Bergvall's Foundation, Novo Nordisk Foundation, the Swedish Diabetes Association and the Swedish Research Council (32X-14643, 32BI-15333, 32P-15439 and 12X-6240). Author contribution: A.W.: experiment design, microscopy data collection and analysis, manuscript writing; J.S.: RT-PCR; A.T.: conception and design, manuscript writing.

Supplementary material available online at
http://jcs.biologists.org/cgi/content/full/123/9/1492/DC1

References

Axelrod, D. (2008). Total internal reflection fluorescence microscopy. *Methods Cell Biol.* **89**, 169-221.

Balla, A. and Balla, T. (2006). Phosphatidylinositol 4-kinases: old enzymes with emerging functions. *Trends Cell Biol.* **16**, 351-361.

Balla, A., Tuymetova, G., Tsiomenko, A., Varnai, P. and Balla, T. (2005). A plasma membrane pool of phosphatidylinositol 4-phosphate is generated by phosphatidylinositol 4-kinase type-III alpha: studies with the PH domains of the oxysterol binding protein and FAPP1. *Mol. Biol. Cell* **16**, 1282-1295.

Balla, A., Kim, Y. J., Varnai, P., Szentpetery, Z., Knight, Z., Shokat, K. M. and Balla, T. (2008). Maintenance of hormone-sensitive phosphoinositide pools in the plasma membrane requires phosphatidylinositol 4-kinase IIIα. *Mol. Biol. Cell* **19**, 711-721.

Berridge, M. J. and Irvine, R. F. (1984). Inositol trisphosphate, a novel second messenger in cellular signal transduction. *Nature* **312**, 315-321.

Biden, T. J., Peter-Riesch, B., Schlegel, W. and Wollheim, C. B. (1987). Ca^{2+}-mediated generation of inositol 1,4,5-triphosphate and inositol 1,3,4,5-tetrakisphosphate in pancreatic islets. Studies with K^+, glucose, and carbamylcholine. *J. Biol. Chem.* **262**, 3567-3571.

Cantley, L. C. (2002). The phosphoinositide 3-kinase pathway. *Science* **296**, 1655-1657.

Czech, M. P. (2003). Dynamics of phosphoinositides in membrane retrieval and insertion. *Annu. Rev. Physiol.* **65**, 791-815.

D'Angelo, G., Vicinanza, M., Di Campli, A. and De Matteis, M. A. (2008). The multiple roles of PtdIns(4)P - not just the precursor of PtdIns(4,5)P2. *J. Cell Sci.* **121**, 1955-1963.

de Barry, J., Janoshazi, A., Dupont, J. L., Procksch, O., Chasserot-Golaz, S., Jeromin, A. and Vitale, N. (2006). Functional implication of neuronal calcium sensor-1 and phosphoinositol 4-kinase-beta interaction in regulated exocytosis of PC12 cells. *J. Biol. Chem.* **281**, 18098-18111.

Dowler, S., Currie, R. A., Campbell, D. G., Deak, M., Kular, G., Downes, C. P. and Alessi, D. R. (2000). Identification of pleckstrin-homology-domain-containing proteins with novel phosphoinositide-binding specificities. *Biochem. J.* **351**, 19-31.

Fruman, D. A., Meyers, R. E. and Cantley, L. C. (1998). Phosphoinositide kinases. *Annu. Rev. Biochem.* **67**, 481-507.

Giraud, F., Gascard, P. and Sulpice, J. C. (1988). Stimulation of polyphosphoinositide turnover upon activation of protein kinases in human erythrocytes. *Biochim. Biophys. Acta* **968**, 367-378.

Grapengiesser, E., Gylfe, E. and Hellman, B. (1988). Glucose-induced oscillations of cytoplasmic Ca^{2+} in the pancreatic β-cell. *Biochem. Biophys. Res. Commun.* **151**, 1299-1304.

Gromada, J., Bark, C., Smidt, K., Efanov, A. M., Janson, J., Mandic, S. A., Webb, D. L., Zhang, W., Meister, B., Jeromin, A. et al. (2005). Neuronal calcium sensor-1 potentiates glucose-dependent exocytosis in pancreatic β cells through activation of phosphatidylinositol 4-kinase β. *Proc. Natl. Acad. Sci. USA* **102**, 10303-10308.

Halaszovich, C. R., Schreiber, D. N. and Oliver, D. (2009). Ci-VSP is a depolarization-activated phosphatidylinositol-4,5-bisphosphate and phosphatidylinositol-3,4,5-trisphosphate 5′-phosphatase. *J. Biol. Chem.* **284**, 2106-2113.

Halenda, S. P. and Feinstein, M. B. (1984). Phorbol myristate acetate stimulates formation of phosphatidyl inositol 4-phosphate and phosphatidyl inositol 4,5-bisphosphate in human platelets. *Biochem. Biophys. Res. Commun.* **124**, 507-513.

Hama, H., Schnieders, E. A., Thorner, J., Takemoto, J. Y. and DeWald, D. B. (1999). Direct involvement of phosphatidylinositol 4-phosphate in secretion in the yeast Saccharomyces cerevisiae. *J. Biol. Chem.* **274**, 34294-34300.

Hammond, G. R., Schiavo, G. and Irvine, R. F. (2009). Immunocytochemical techniques reveal multiple, distinct cellular pools of PtdIns4P and PtdIns(4,5)P(2). *Biochem. J.* **422**, 23-35.

Hausser, A., Storz, P., Martens, S., Link, G., Toker, A. and Pfizenmaier, K. (2005). Protein kinase D regulates vesicular transport by phosphorylating and activating phosphatidylinositol-4 kinase IIIβ at the Golgi complex. *Nat. Cell Biol.* **7**, 880-886.

Hay, J. C., Fisette, P. L., Jenkins, G. H., Fukami, K., Takenawa, T., Anderson, R. A. and Martin, T. F. (1995). ATP-dependent inositide phosphorylation required for Ca^{2+}-activated secretion. *Nature* **374**, 173-177.

Hendricks, K. B., Wang, B. Q., Schnieders, E. A. and Thorner, J. (1999). Yeast homologue of neuronal frequenin is a regulator of phosphatidylinositol-4-OH kinase. *Nat. Cell Biol.* **1**, 234-241.

Kapp-Barnea, Y., Melnikov, S., Shefler, I., Jeromin, A. and Sagi-Eisenberg, R. (2003). Neuronal calcium sensor-1 and phosphatidylinositol 4-kinase beta regulate IgE receptor-triggered exocytosis in cultured mast cells. *J. Immunol.* **171**, 5320-5327.

Kardasz, A. M., Thams, P., Capito, K. and Hedeskov, C. J. (1997). Carbamoylcholine regulation of polyphosphoinositide synthesis and hydrolysis in cultured, dispersed, digitonin-permeabilized mouse pancreatic islet cells. *Eur. J. Endocrinol.* **136**, 539-545.

Kontos, C. D., Stauffer, T. P., Yang, W. P., York, J. D., Huang, L., Blanar, M. A., Meyer, T. and Peters, K. G. (1998). Tyrosine 1101 of Tie2 is the major site of association of p85 and is required for activation of phosphatidylinositol 3-kinase and Akt. *Mol. Cell. Biol.* **18**, 4131-4140.

Lemmon, M. A. (2008). Membrane recognition by phospholipid-binding domains. *Nat. Rev. Mol. Cell Biol.* **9**, 99-111.

Levine, T. P. and Munro, S. (1998). The pleckstrin homology domain of oxysterol-binding protein recognises a determinant specific to Golgi membranes. *Curr. Biol.* **8**, 729-739.

Levine, T. P. and Munro, S. (2002). Targeting of Golgi-specific pleckstrin homology domains involves both PtdIns 4-kinase-dependent and -independent components. *Curr. Biol.* **12**, 695-704.

Loyet, K. M., Kowalchyk, J. A., Chaudhary, A., Chen, J., Prestwich, G. D. and Martin, T. F. (1998). Specific binding of phosphatidylinositol 4,5-bisphosphate to calcium-dependent activator protein for secretion (CAPS), a potential phosphoinositide effector protein for regulated exocytosis. *J. Biol. Chem.* **273**, 8337-8343.

Martin, T. F. (2001). PI(4,5)P_2 regulation of surface membrane traffic. *Curr. Opin. Cell Biol.* **13**, 493-499.

Miyazaki, J., Araki, K., Yamato, E., Ikegami, H., Asano, T., Shibasaki, Y., Oka, Y. and Yamamura, K. (1990). Establishment of a pancreatic beta cell line that retains glucose-inducible insulin secretion: special reference to expression of glucose transporter isoforms. *Endocrinology* **127**, 126-132.

Nakanishi, S., Catt, K. J. and Balla, T. (1995). A wortmannin-sensitive phosphatidylinositol 4-kinase that regulates hormone-sensitive pools of inositolphospholipids. *Proc. Natl. Acad. Sci. USA* **92**, 5317-5321.

Olsen, H. L., Høy, M., Zhang, W., Bertorello, A. M., Bokvist, K., Capito, K., Efanov, A. M., Meister, B., Thams, P., Yang, S. N. et al. (2003). Phosphatidylinositol 4-kinase serves as a metabolic sensor and regulates priming of secretory granules in pancreatic β cells. *Proc. Natl. Acad. Sci. USA* **100**, 5187-5192.

Rhee, S. G. and Choi, K. D. (1992). Regulation of inositol phospholipid-specific phospholipase C isozymes. *J. Biol. Chem.* **267**, 12393-12396.

Roy, A. and Levine, T. P. (2004). Multiple pools of phosphatidylinositol 4-phosphate detected using the pleckstrin homology domain of Osh2p. *J. Biol. Chem.* **279**, 44683-44689.

Rozen, S. and Skaletsky, H. (2000). Primer3 on the WWW for general users and for biologist programmers. *Methods Mol. Biol.* **132**, 365-386.

Speidel, D., Salehi, A., Obermüller, S., Lundquist, I., Brose, N., Renström, E. and Rorsman, P. (2008). CAPS1 and CAPS2 regulate stability and recruitment of insulin granules in mouse pancreatic β-cells. *Cell Metab.* **7**, 57-67.

Stauffer, T. P., Ahn, S. and Meyer, T. (1998). Receptor-induced transient reduction in plasma membrane PtdIns(4,5)P_2 concentration monitored in living cells. *Curr. Biol.* **8**, 343-346.

Steyer, J. A. and Almers, W. (2001). A real-time view of life within 100 nm of the plasma membrane. *Nat. Rev. Mol. Cell Biol.* **2**, 268-275.

Tamarina, N. A., Kuznetsov, A., Rhodes, C. J., Bindokas, V. P. and Philipson, L. H. (2005). Inositol (1,4,5)-trisphosphate dynamics and intracellular calcium oscillations in pancreatic β-cells. *Diabetes* **54**, 3073-3081.

Taylor, M. V., Metcalfe, J. C., Hesketh, T. R., Smith, G. A. and Moore, J. P. (1984). Mitogens increase phosphorylation of phosphoinositides in thymocytes. *Nature* **312**, 462-465.

Teruel, M. N., Blanpied, T. A., Shen, K., Augustine, G. J. and Meyer, T. (1999). A versatile microporation technique for the transfection of cultured CNS neurons. *J. Neurosci. Methods* **93**, 37-48.

Thore, S., Dyachok, O. and Tengholm, A. (2004). Oscillations of phospholipase C activity triggered by depolarization and Ca^{2+} influx in insulin-secreting cells. *J. Biol. Chem.* **279**, 19396-19400.

Thore, S., Dyachok, O., Gylfe, E. and Tengholm, A. (2005). Feedback activation of phospholipase C via intracellular mobilization and store-operated influx of Ca^{2+} in insulin-secreting β-cells. *J. Cell Sci.* **118**, 4463-4471.

Thore, S., Wuttke, A. and Tengholm, A. (2007). Rapid turnover of phosphatidylinositol-4,5-bisphosphate in insulin-secreting cells mediated by Ca^{2+} and the ATP-to-ADP ratio. *Diabetes* **56**, 818-826.

Varnai, P. and Balla, T. (1998). Visualization of phosphoinositides that bind pleckstrin homology domains: calcium- and agonist-induced dynamic changes and relationship to myo-[^{3}H]inositol-labeled phosphoinositide pools. *J. Cell Biol.* **143**, 501-510.

Walch-Solimena, C. and Novick, P. (1999). The yeast phosphatidylinositol-4-OH kinase pik1 regulates secretion at the Golgi. *Nat. Cell Biol.* **1**, 523-525.

Waselle, L., Gerona, R. R., Vitale, N., Martin, T. F., Bader, M. F. and Regazzi, R. (2005). Role of phosphoinositide signaling in the control of insulin exocytosis. *Mol. Endocrinol.* **19**, 3097-3106.

Wiedemann, C., Schäfer, T. and Burger, M. M. (1996). Chromaffin granule-associated phosphatidylinositol 4-kinase activity is required for stimulated secretion. *EMBO J.* **15**, 2094-2101.

Xu, C., Watras, J. and Loew, L. M. (2003). Kinetic analysis of receptor-activated phosphoinositide turnover. *J. Cell Biol.* **161**, 779-791.

Yin, H. L. and Janmey, P. A. (2003). Phosphoinositide regulation of the actin cytoskeleton. *Annu. Rev. Physiol.* **65**, 761-789.

Yu, J. W., Mendrola, J. M., Audhya, A., Singh, S., Keleti, D., DeWald, D. B., Murray, D., Emr, S. D. and Lemmon, M. A. (2004). Genome-wide analysis of membrane targeting by S. cerevisiae pleckstrin homology domains. *Mol. Cell* **13**, 677-688.

Zhao, X., Varnai, P., Tuymetova, G., Balla, A., Toth, Z. E., Oker-Blom, C., Roder, J., Jeromin, A. and Balla, T. (2001). Interaction of neuronal calcium sensor-1 (NCS-1) with phosphatidylinositol 4-kinase beta stimulates lipid kinase activity and affects membrane trafficking in COS-7 cells. *J. Biol. Chem.* **276**, 40183-40189.

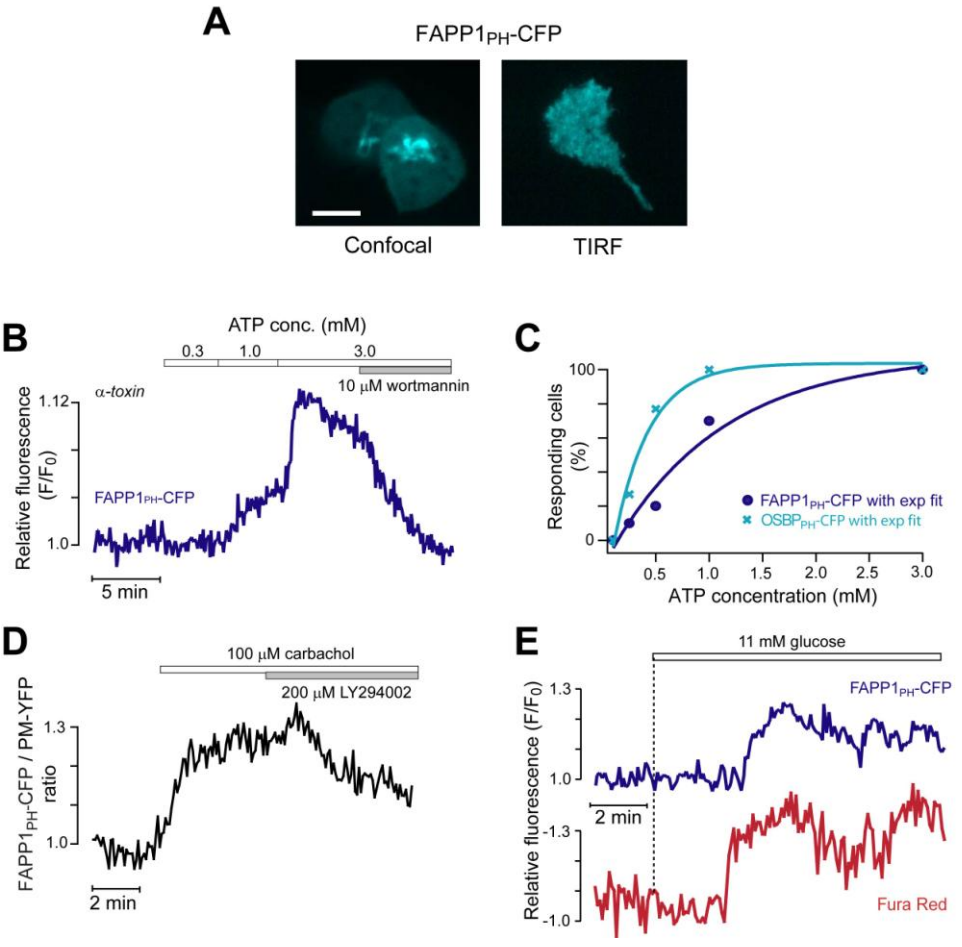
A
FAPP1PH-CFP
Confocal
TIRF
B
ATP conc. (mM)
0.3
1.0
3.0
10 μM wortmannin
α-toxin
Relative fluorescence (F/F0)
1.12
1.0
FAPP1PH-CFP
5 min
C
Responding cells (%)
100
0
FAPP1PH-CFP with exp fit
OSBPPH-CFP with exp fit
0.5
1.0
1.5
2.0
2.5
3.0
ATP concentration (mM)
D
100 μM carbachol
200 μM LY294002
FAPP1PH-CFP / PM-YFP ratio
1.3
1.0
2 min
E
11 mM glucose
FAPP1PH-CFP
Relative fluorescence (F/F0)
1.3
1.0
2 min
-1.3
-1.0
Fura Red